THE EFFECT OF BREAKING GRAVITY WAVES ON THE DYNAMICS AND CHEMISTRY OF THE MESOSPHERE AND LOWER THERMOSPHERE
(Invited Review)

Rolando R. Garcia
National Center for Atmospheric Research*
P.O. Box 3000
Boulder, Colorado 80307

The influence of breaking gravity waves on the dynamics and chemical composition of the 60-110 km region is investigated with a two-dimensional model that includes a parameterization of gravity wave momentum deposition and diffusion.

The dynamical model is that described by Garcia and Solomon (1983) and Solomon and Garcia (1983) and includes a complete chemical scheme for the mesosphere and lower thermosphere. The paramaterization of Lindzen (1981) is used to calculate the momentum deposited and the turbulent diffusion produced by the gravity waves.

It is found that wave momentum deposition drives a very vigorous mean meridional circulation, produces a very cold summer mesopause and reverses the zonal wind jets above about 85 km (Fig. 1). The momentum deposition and turbulent diffusion are much weaker at equinox than at solstice (Fig. 2). In Figure 3 the seasonal variation of the turbulent diffusion coefficient is consistent with the behavior of mesospheric turbulence inferred from MST radar echoes (Balsley et al., 1983; see Fig. 3 a, b).

The large decreases in turbulent diffusion at the equinoxes have profound effects on the distribution of certain chemical trace species. In particular, atomic oxygen in the lower thermosphere increases at the equinoxes because loss through diffusion into the sink region below $\simeq 90$ km is reduced. This increase in atomic oxygen is reflected in the greater intensity of the 5577 Å green line airglow emission. The model reproduces very well the observed seasonal variation of the green line airglow (Fig. 4).

Ozone in the upper mesosphere is destroyed efficiently by HO_x (H + OH + HO_2) catalysis. HO_x abundance at the 80 km level depends sensitively on the concentration of water vapor, which in turn is determined by upward diffusion from the lower mesosphere. At equinox, the diffusive flux of H_2O is reduced, HO_x abundances decrease and O_3 increases in the upper mesosphere. The 1.27 μm O_2 airglow is a proxy for O_3 abundances at 80 km. Fig. 5 shows that the model reproduces the major features of the seasonal variation of 1.27 μm airglow observed by the SME satellite (Thomas et al., 1984).

In conclusion, the large degree of consistency between model results and various types of dynamical and chemical data supports very strongly the hypothesis that breaking gravity waves play a major role in determining the zonally-averaged dynamical and chemical structure of the 60-110 km region of the atmosphere. A detailed account of this work is given in Garcia and Solomon (1984).

REFERENCES

Balsley, B. B., W. L. Ecklund, and D. C. Fritts, 1983: VHF echoes from the high-latitude mesosphere and lower thermosphere: Observations and interpretations, *J. Atmos. Sci.,* *40,* 2451-2466.

Cogger, L. L., R. D. Elphinstone, and J. S. Murphree, 1981: Temporal and latitudinal 5577Å airglow variations. *Can. J. Phys., 59,* 1296-1307.

Garcia, R. R., and S. Solomon, 1983: A numerical model of the zonally-averaged dynamical and chemical structure of the middle atmosphere. *J. Geophys. Res., 88,* 1379-1400.

Garcia, R. R., and S. Solomon, 1984: The effect of breaking gravity waves on the dynamics and chemical composition of the mesosphere and lower thermosphere, *J. Geophys. Res.* (submitted).

Lindzen, R. S., 1981: Turbulence and stress owing to gravity wave and tidal breakdown. *J. Geophys. Res., 86,* 9707-9714.

Solomon, S., and R. R. Garcia, 1983: On the distribution of nitrogen dioxide in the high latitude stratosphere. *J. Geophys. Res., 88,* 5229-5239.

Thomas, R. J., C. A. Barth, and S. Solomon, 1984: Seasonal variations of ozone in the upper mesosphere and gravity waves. *Geophys. Res. Lett.,* (in press).
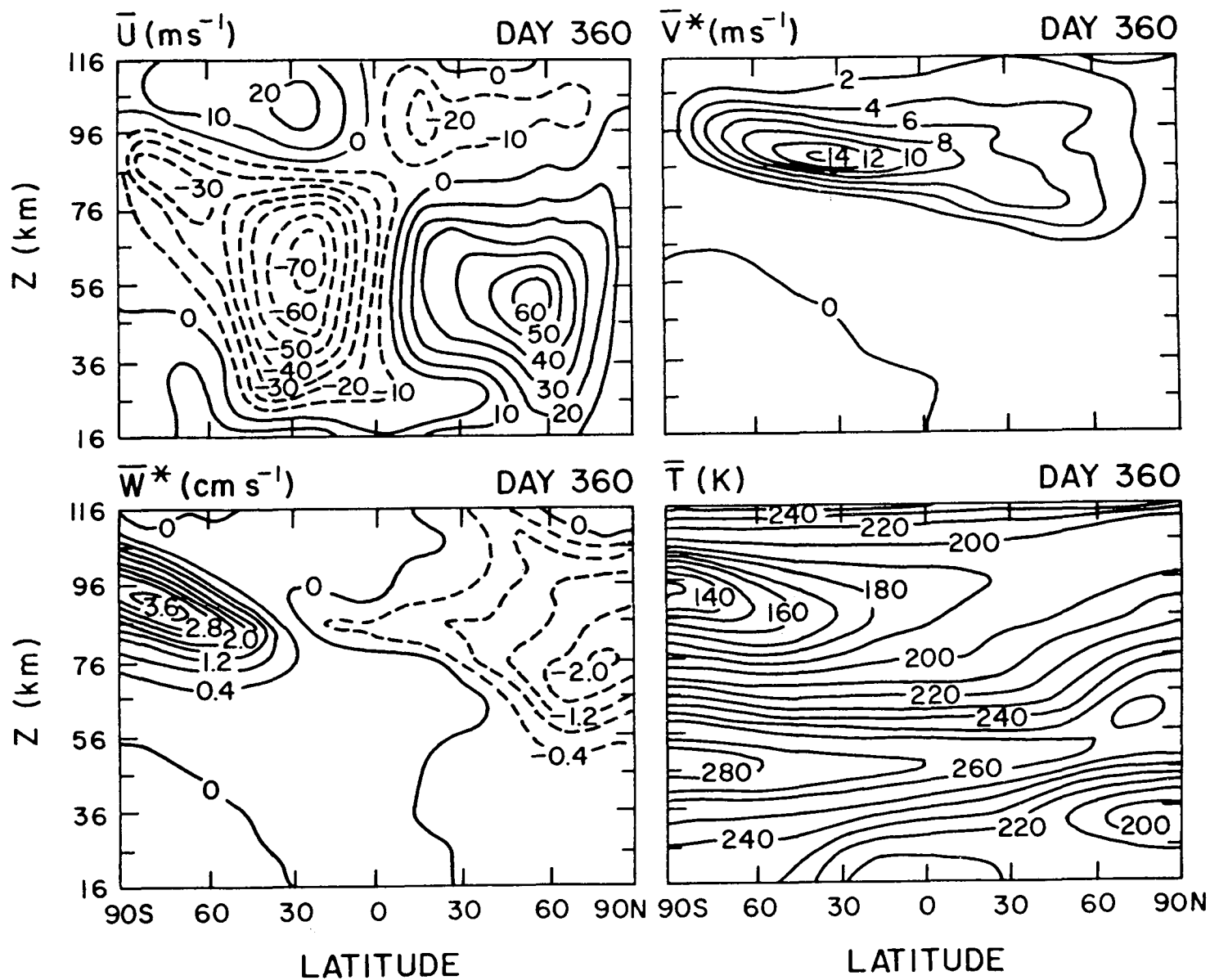
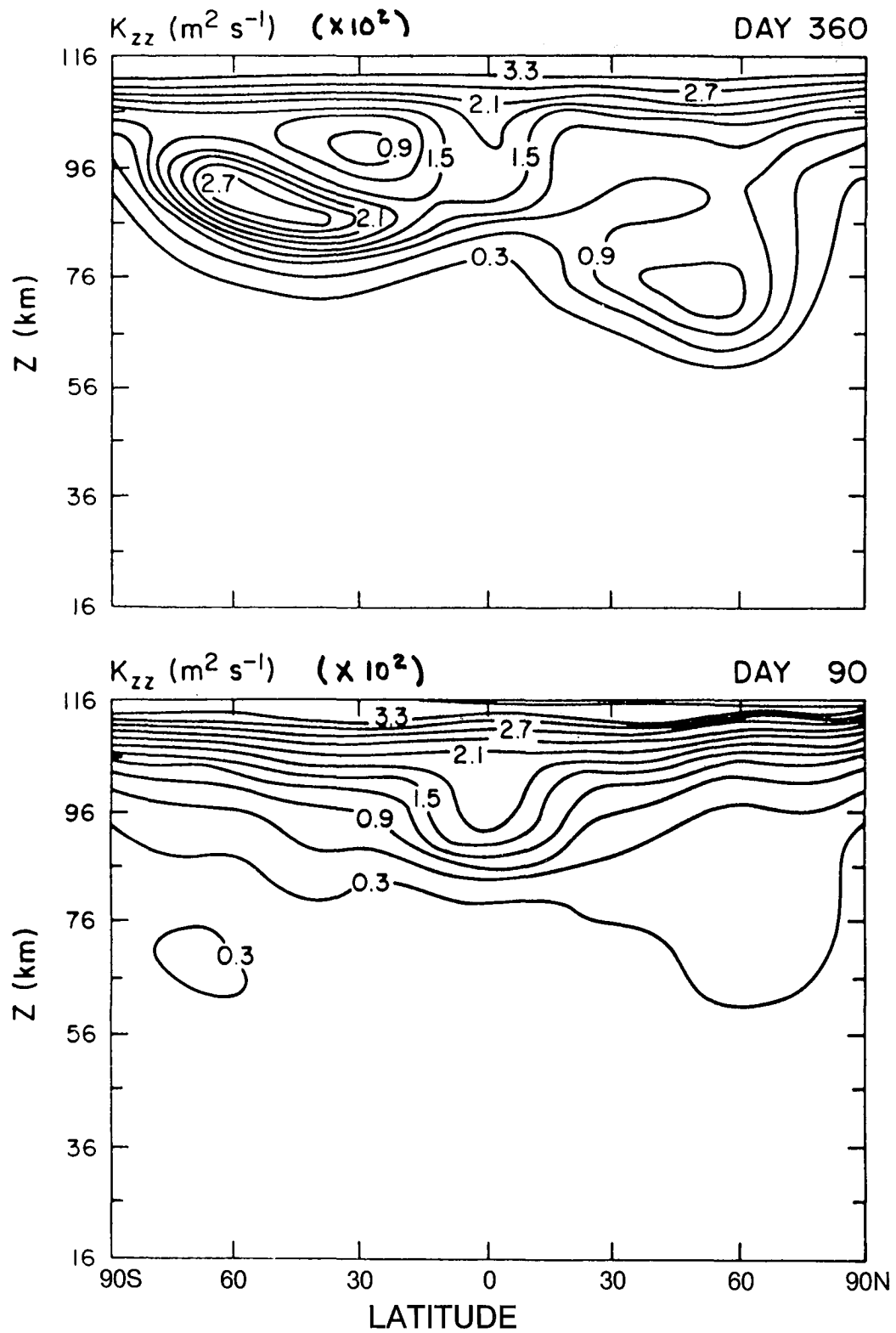Figure 1. Zonally averaged circulation and temperature for model northern hemisphere winter solstice.

Figure 2. Vertical eddy diffusion coefficient due to breaking gravity waves for solstice and equinox.
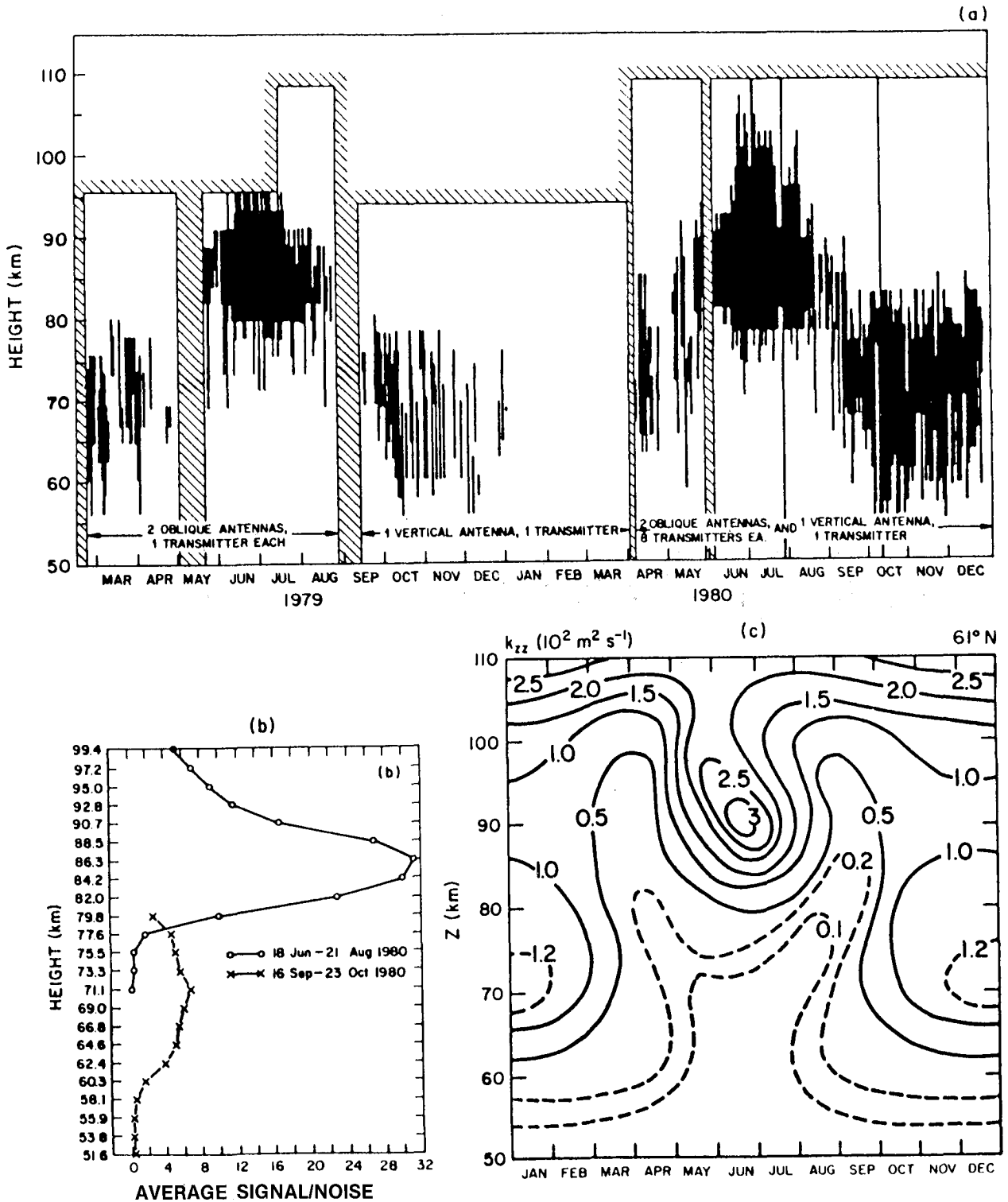
Figure 3. (a) Height distribution of MST radar echoes at Poker Flat (65 °N) as a function of season. Cross-hatched areas denote periods and altitudes for which no data are available. (From Balsley *et al.*, 1983). (b) Vertical profiles of radar echo signal-to-noise ratio for summer (June 18-August 21, 1980 average) and fall (September 16-October 23, 1980). (Balsley *et al.*, 1983). (c) Seasonal variation of the turbulent diffusion coefficient at 61 ° north latitude.
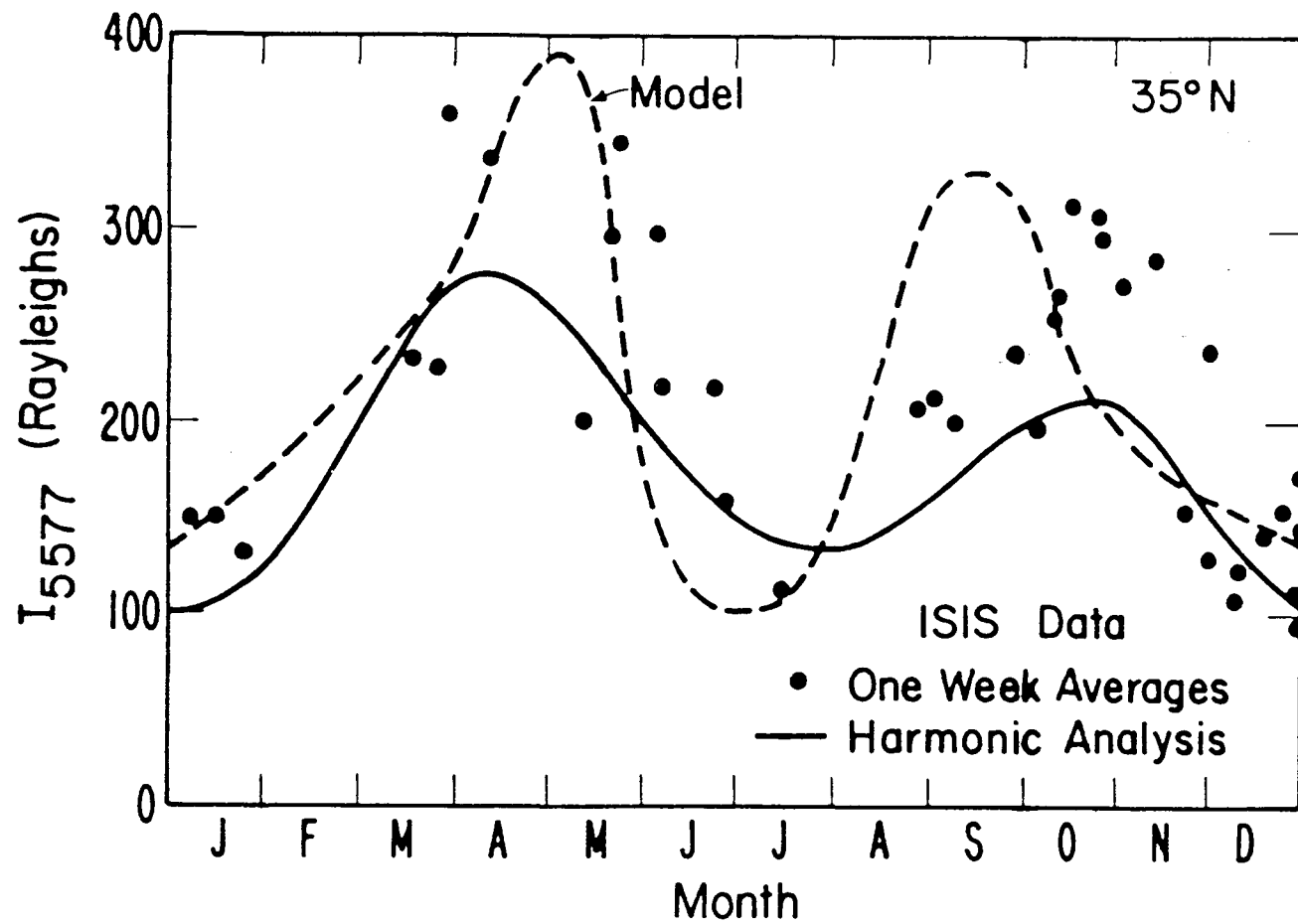
101

Figure 4. Seasonal variation of the atomic oxygen green line (5577 Å) emission intensities observed by the ISIS satellite at 35 °N adapted from (Cogger *et al.*, 1981) compared with model calculations.
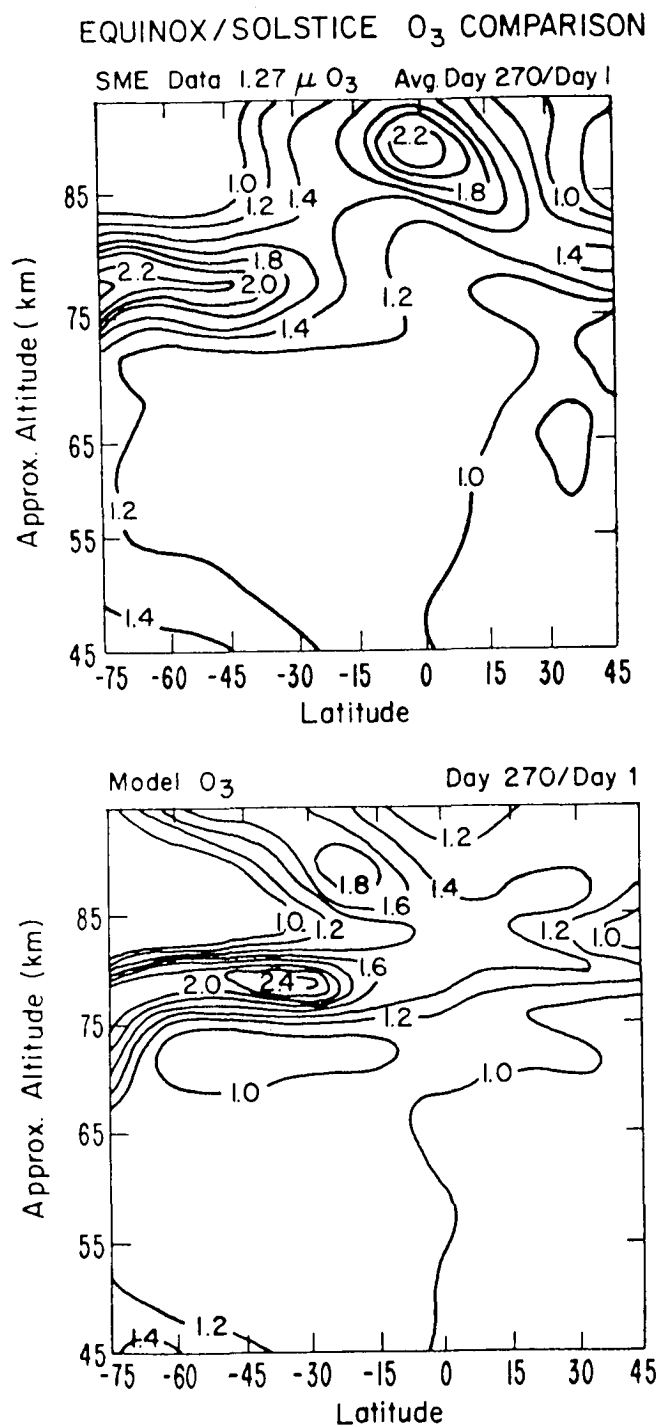
EQUINOX/SOLSTICE O_3 COMPARISON

Figure 5. Top panel: Ratio of O_3 observations by the Solar Mesosphere Explorer satellite (Thomas *et al.*, 1984) for one week averages about day 270 to day 1 (southern hemisphere spring/summer; northern hemisphere fall/winter). Bottom panel: Same, as computed by the model.

103